

Validation of the utilisation of automatic placement of anatomical and sliding landmarks on three-dimensional models for shape analysis of human pelves

T.M. Mbonani ^a, A.C. Hagg ^a, E.N. L'Abbé ^a, A.C. Oettlé ^{a,b}, A.F. Ridel ^{a,*}

^aDepartment of Anatomy, University of Pretoria, Private Bag x323, Arcadia, 0007, South Africa

^bAnatomy and Histology Department, School of Medicine, Sefako Makgatho Health Sciences University, Ga-Rankuwa, Pretoria, South Africa

*Corresponding author. Email: Alisonridel66@gmail.com

Highlights

- The application of automatic landmarking in forensics can increase objectivity and reliability.
- Three-dimensional tools may be a valuable alternative to analyse sex-related skeletal variation.
- Automatic landmarking reduces measurement errors, in addition to quantifying sex differences.

Abstract

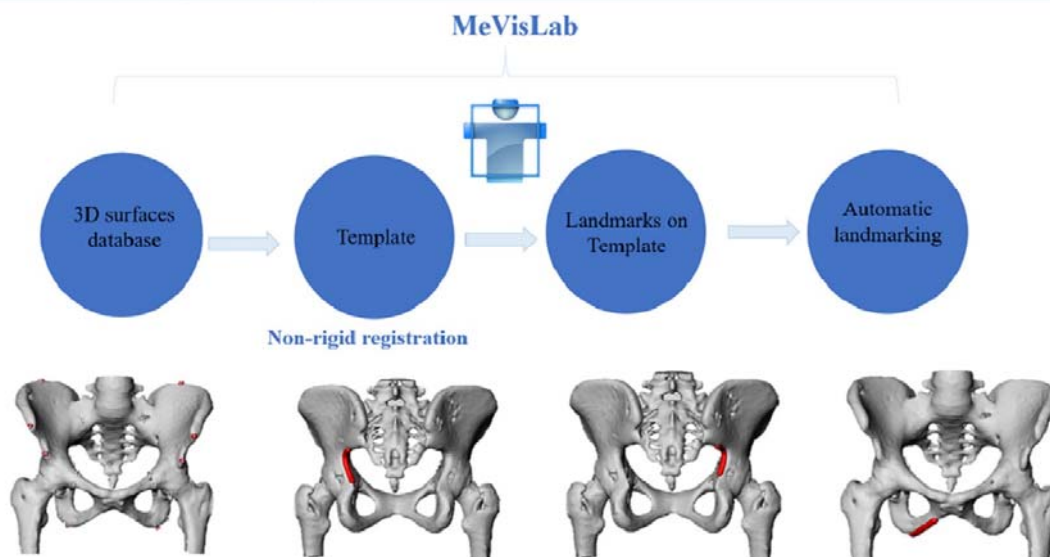
Estimating sex from unknown human skeletal remains is an important component in forensic anthropology. Currently, both morphological and morphometric methods are used for sex estimation. These methods employ landmarks to make morphological comparisons between and within groups. Manual landmarking has been regarded as time-consuming and subjective. To decrease observer subjectivity and reduce measurement errors, an automated three-dimensional (3D) method was developed. This study aimed to validate the utilisation of the automatic placement of anatomical and sliding landmarks on 3D pelvis models for shape analysis using Computed Tomography (CT) scans.

Computed Tomography scans of adult South Africans were obtained from Steve Biko Academic Hospital, Pretoria, South Africa. In this study, automatic landmarking was validated on 130 3D reconstructions of the adult human pelvis. Eighteen anatomical and 260 sliding landmarks were registered on 130 3D models of the same individuals manually and automatically using the MeVisLab © v 2.7.1 software. Landmark datasets were acquired using both landmarking methods and compared using reproducibility testing and geometric morphometric (GMM) analysis. Reproducibility testing of both landmark datasets demonstrated minimal dispersion errors (<2 mm), indicating the reliability and repeatability of both landmarking methods. Variance analysis showed that pelvis shape sex-related variation was statistically significant ($p < 0.05$) using both methods. In addition, cross-validated discriminant function analysis (DFA) yielded accuracies between 82.98 – 97.73% and 65.91 – 93.18% using automatic and manual placement of landmarks, respectively.

In forensics using 3D automatic approaches, and advanced statistical analysis might allow forensic anthropologists to estimate sex in a more accurate and repeatable way.

Graphical abstract

How accurate is the utilisation of automatic placement of anatomical and sliding landmarks on three-dimensional models for shape analysis of human pelvises?



Keywords: Computed tomography (CT) scans; 3D reconstructions; Anatomical and sliding landmarks; Automatic landmarking approach; Geometric morphometric methods (GMM); 3D sex estimation

Introduction

The identification of unknown persons in South Africa is a challenge due to, among other reasons, its high influx of migrant and illegal labourers and the vast number of unidentified remains found in the country each year [1]. For example, in 2021, state mortuaries in only one of the country's nine provinces (Gauteng) reported 1173 unidentified bodies for 2020 [2]. In 2008, an entity within the University of Pretoria, South Africa, was established to assist in identifying unknown skeletal remains by means of estimating a biological profile and interpreting traumatic injury to bone and pathology. As the expression of sexual dimorphism is highly population-specific [3], sex estimation becomes a foremost step in developing a reliable biological profile in the South African context.

Sex estimation techniques focus on the pelvis's morphological and long bones' metric variations [4]. However, to a greater degree, sex estimation techniques are primarily utilized in the human bony pelvis due to the presence of reproductive differences between males and females. The accuracy and reliability of sex estimation depend directly on the completeness and state of preservation of the skeletal remains and the degree of clarity of features present [5]. The pubic bone is the most sexually dimorphic feature of the bony pelvis; however, it is not often recovered intact. Therefore, it is necessary to improve scientific reliability to extract biologically important information accurately from more than one skeletal element. Morphological (e.g., scoring analysis) and morphometric methods (e.g., Linear Discriminant Function Analysis (LDFA)) have been applied to the cranium and postcrania to estimate the biological profile of unknown individuals based on a South African custom database [6,7]. The morphometric methods involve a suite of bone measurements for various metric analyses,

including Linear Discriminant Function Analysis (LDFA). However, the morphological approach has been criticized extensively due to the subjectivity involved, and the reliability of the method depends on the observer's experience [5]. LDFA is the most widely used morphometric approach and appears more reliable; however, it becomes difficult to use this technique when all the necessary measurements are not assessable. This limitation could be significantly overcome by geometric morphometrics (GMM).

GMM focuses on biological shape analysis using cartesian coordinates (x, y, z) of anatomical landmarks [8]. The utilisation of GMM for sex estimation using the pelvis may be preferable to morphometric methods because they retain the objects' geometry and analyse subtle differences among structures [8]. Furthermore, GMM could significantly overcome the exclusion of fragmented pelvises in sex estimation analysis by creating discriminant shape matrices to analyse specific patterns not readily revealed by traditional methods.

Following the expansion of new 3D imaging technologies, researchers have developed morpho-phenotyping shape analysis tools using automatic landmarking and semi-landmarking for forensic case analysis [9]. New 3D imaging methods may permit forensic anthropologists to assess specific sexual dimorphism patterns not readily revealed by morphological and morphometric methods. Furthermore, 3D imaging approaches involving practical 3D scanning modalities, accurate 3D anatomical information extraction, and advanced statistical analysis may allow forensic anthropologists to estimate sex and analyse pelvis-shape-related variation more accurately and repeatably. Ultimately, 3D imaging approaches may provide forensic anthropologists with a more efficient and improved way of estimating the biological profile. Current morphometric approaches for sex estimation almost exclusively rely on conventional craniometric measures derived from 3D point landmarks that are mostly manually placed. Such manual placements of landmarks are extremely time-consuming on large 3D surface samples and may induce observer subjectivity and error in placing these landmarks [10]. These limitations may be overcome by applying the automatic landmarking method developed by Ridel and colleagues [10,11], offering increased objectivity or consistency and the possibility of standardisation. This study aimed to validate the use of the automatic placement of anatomical and sliding landmarks on 3D models for shape analysis of human pelvis. This study is the first attempt at validating the application of the automatic placement of anatomical and sliding landmarks on 3D reconstructions of the human bony pelvis to analyse variations related to the pelvis shape of South Africans.

Materials and methods

Materials

The sample consisted of 130 adult CT scans (48 males and 82 females) collected retrospectively at Steve Biko Academic Hospital, Pretoria, South Africa. The anonymous patients were scanned in a supine position using a Siemens Somatom Sensation 64-slice Computed Tomography scanner with a slice thickness of 0.5 mm and a matrix of 512×512 pixels. All the reconstructed data were saved in the Digital Imaging and Communications in Medicine (DICOM) format. The overall age ranged between 18 and 80 years. All patient data used in the study were anonymised, with only the biological information pertinent to the current study recorded for analysis (sex). For consistency during data collection, any condition that could affect the morphology of the 3D reconstructed pelvis and subsequent results was removed from the sample. Such conditions include any pathologies, trauma, surgical intervention, or deformities. Ethical clearance was obtained from the Research Ethics

Committee of the Faculty of Health Sciences of the University of Pretoria (Ethics Reference No:253/2021).

Methods

Segmentation and construction of 3D meshes

The 130 CT datasets obtained were segmented using the Edit New Label field module of Avizo 2019.3 software (Thermo Fisher Scientific, Inc.). The threshold values between segmented components were obtained according to the “Half Maximum Height” (HMH) quantitative iterative thresholding method [12] using ImageJ software [13]. The bone material was then partitioned and extracted from other materials (e.g., artefacts and air) or noise present in the scab. The segmentation resulted in the generation of 3D reconstructions of the pelvis saved in polygon file format (.ply).

Landmarks and sliding landmarks

Anatomical landmarks are defined by specific biological structures and are thus consistent across all individuals of a species. In this study, the standard anatomical and semi-landmarks were designed to reflect the pelvis shape in the best possible manner, resulting in a total of 18 anatomical (Table 1) and 260 sliding landmarks (Table 2). In addition, four sets of semi-landmarks (curve1: 68), (curve 2: 68), (curve 3: 62), and (curve 4: 62) were placed using an interpolation algorithm of 1 mm to capture the two anatomical features bilaterally named the greater sciatic notches and ischio-pubic rami. The *MeVisLab 2.7.1* software was used for manually and automatically placing the anatomical and sliding landmarks. The landmarks placed manually and automatically on 3D models of the pelvis are depicted in Fig. 1. While manual landmarking involves localising landmarks manually on 3D reconstructions, the automatic landmarking procedure used for this study was firstly introduced by Claes [14], and recently tested and published by Ridel and colleagues [10]. Ridel and colleagues [10] applied this non-rigid generic mesh-to-mesh matching algorithm, known as the automatic landmarking method, to accurately extract and analyse anatomical areas from 3D models using an extensive database of CBCT scans of modern South Africans [10,11]. The adapted workflow of the automatic landmarking used in this research on a 3D model of the pelvis is depicted in Fig. 2.

Table 1. Definition, abbreviation and nature of anatomical landmarks used [15,16].

Landmarks	Abbreviation	Nature	Definition
1/2-Anterior superior iliac spine	ASIS	Bilateral	Anterior end of the iliac crest
3/4-Anterior inferior iliac spine	AIIS	Bilateral	Bony prominence on the anterior border of the ilium forming the superior border of the acetabulum
5/6-Posterior superior iliac spine	PSIS	Bilateral	Posterior terminus of the iliac crest
7/8-Iliac crest		Bilateral	Superior border of the ilium
9/10-Ischial spine	IS	Bilateral	Projection inferior to the greater sciatic notch
11/14-Superior point on ischial tuberosity	IIT	Bilateral	Most superior point on the blunt, rough, massive postero-inferior corner of the os coxa
12/15-Inferior point of ischial tuberosity	IIT	Bilateral	Most inferior point on the blunt, rough, massive postero-inferior corner of the os coxae
13/16-Distal point on ischial tuberosity	IIT	Bilateral	Most distal point on the blunt, rough, massive postero-inferior corner of the os coxae
17/18-Arcuate line	AL	Bilateral	Elevation that sweeps antero-inferiorly across the medial surface of the os coxae from the apex of the auricular surface toward the pubis

Table 2. Definition, abbreviation and nature of pelvis sliding landmarks used [15,16].

Landmarks	Abbreviation	Nature	Definition
Greater sciatic notch	GSN	Bilateral	Wide notch inferior to the posterior inferior iliac spine
Ischio-pubic ramus	IPR	Bilateral	Thin, flat strip of bone connecting the pubis to the ischium

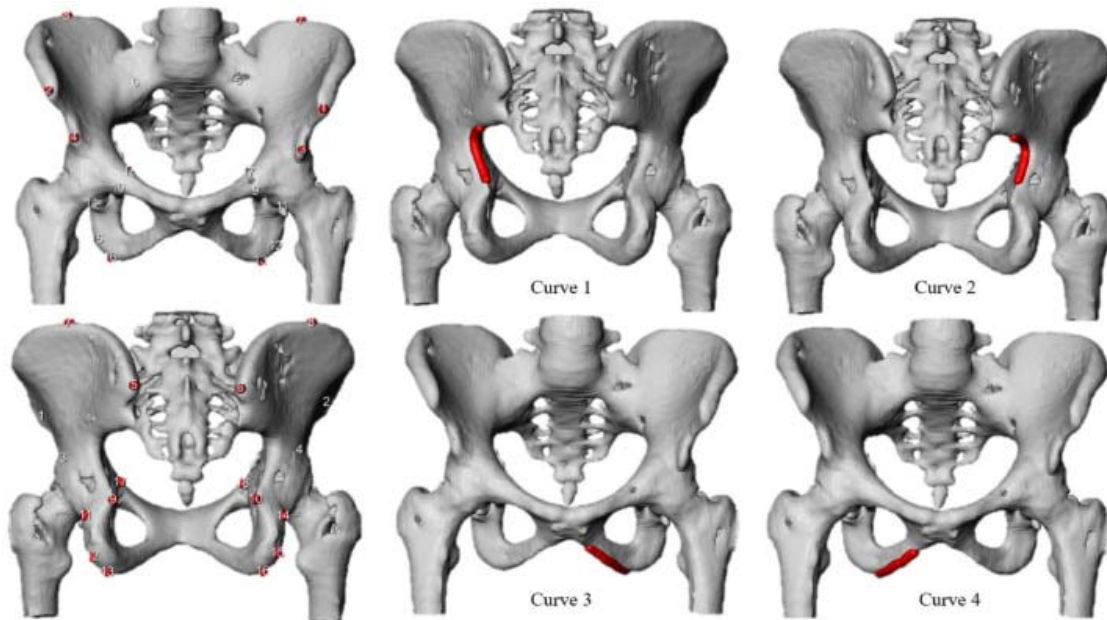


Fig. 1. Anatomical and semi-landmarks localized on a 3D pelvis model [15,16]

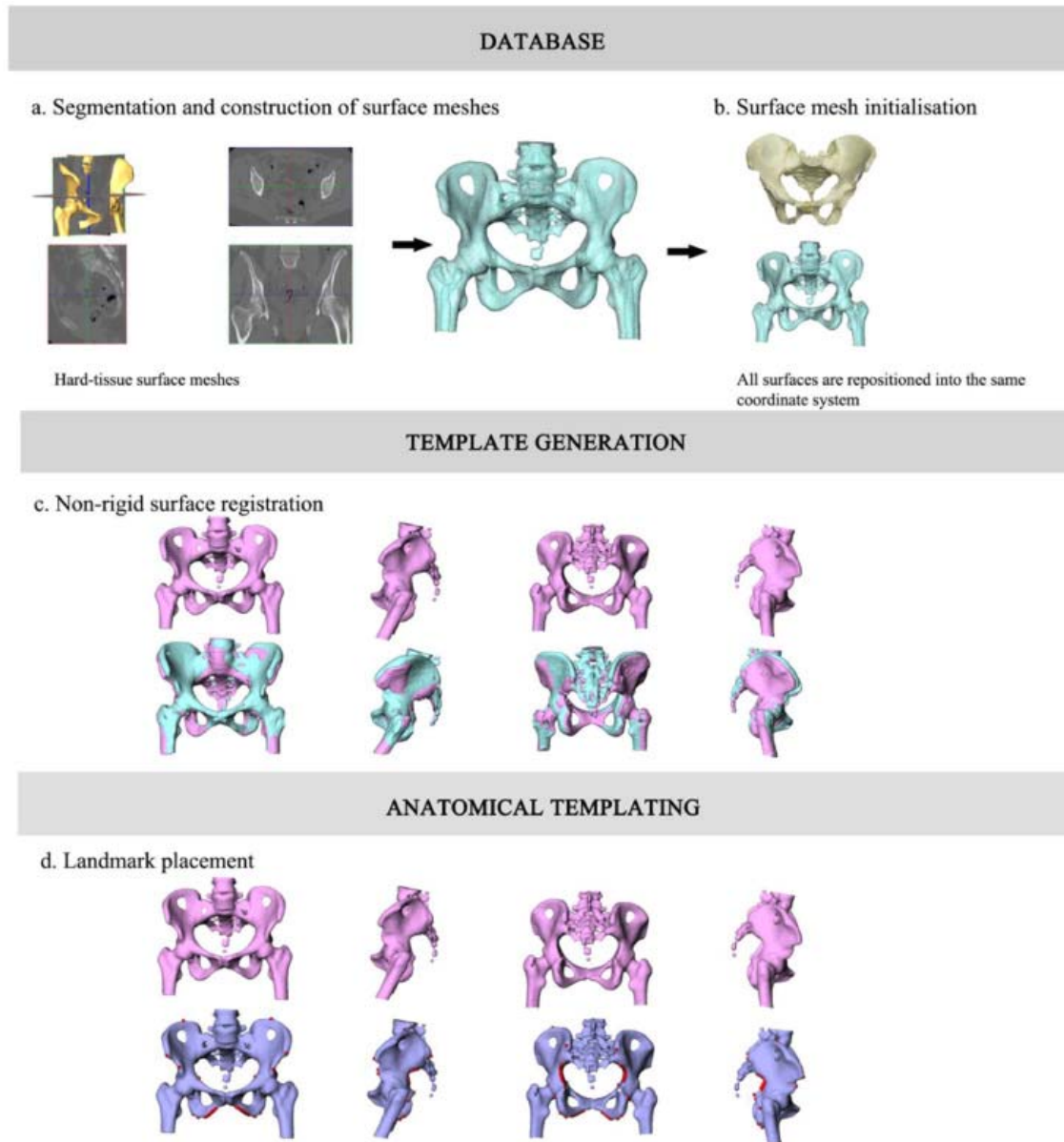


Fig. 2. Workflow of automatic landmarking procedure (pelvis). a: Segmentation and construction of surface meshes; b: Surface mesh initialisation; c: Non-rigid surface registration; d: Landmark placements on templates [10].

Statistical analysis

Validating the automatic landmarking method on 3D pelvis models

To assess the reproducibility of the automatic placement of anatomical and sliding landmarks, intra- and inter-observer errors between both landmarking methods were compared. To compare intra- observer errors (INTRA-OE) and inter-observer errors (INTER-OE), ten scans were randomly selected from the sample. To assess the reproducibility of the landmarks for INTRA-OE and INTER-OE, the placement of landmarks was performed by the same observer and by two different observers within an interval of two weeks, respectively.

In this study, to assess the reproducibility of the 18 anatomical and 260 sliding landmark matrices, dispersion was used. Dispersion calculates the mean distance between the mean placement of the landmarks and all following landmark placements, underlining any frequently erroneous landmarks. The dispersion (Δ_{ij}) for each landmark i and individual j was used to calculate each landmark's reproducibility. Dispersion is defined as the Mean Euclidean Distance (MED) of the sample landmark p_{ijk} to the mean \bar{p}_{ij} of the (x,y,z)-coordinates of landmark i over all observations k (inter, intra, resp.) for subject j (Formula 1):

$$\Delta_{ij} = \sum_{k=1}^K \frac{\|p_{ijk} - \bar{p}_{ij}\|}{K}, \text{ with } \bar{p}_{ij} = \sum_{k=1}^K \frac{p_{ijk}}{K} \quad (1)$$

Global precision was observed as the global (averaged over all landmarks) mean ($\mu\Delta$) and median ($m\Delta$) of the mean ($\mu\Delta_i$) and median ($m\Delta_i$) values per landmark over all subjects.

Comparison of sex estimation analysis using geometric morphometric methods

A sex estimation analysis on matrices acquired from both landmarking procedures was visualised and quantified through the application of geometric morphometric methods (GMM), and the results were then compared. A Generalised Procrustes Analysis (GPA) was performed on the cartesian coordinates resulting from the manual and automatic procedures to obtain orientation-invariant shape coordinates [17,18]. GPA translates and rotates each specimen to minimise the squared, summed distances (squared Procrustes distance) between corresponding landmarks on each configuration and an iteratively computed mean configuration [17]. More precisely, GPA is primarily by which shape variables are obtained from landmark data [19,20]. A principal component analysis (PCA) was performed to assess sex-related shape variations between both methods using independent transformed variables referred to as principal component (PC) scores. PCA is a dimension-reduction technique that identifies orthogonal linear combinations of the original variables that most efficiently reproduce sample variability [17]. Essentially, PCA provides insight into the covariation between the shape variables. Before statistical testing is applied, a multivariate normality test was conducted to analyse the PC scores distribution through the interpretation of Q-Q plots to allow the presumption that the variables were normally distributed [21]. Parametric and non-parametric testing was used to double-check the results, and the results were considered reliable if both tests provided a similar outcome. To assess the influence of sex on pelvis shape variation, a parametric test: Multiple Analysis of Variance (MANOVA) and two non-parametric tests: 50-50 MANOVA and permutation testing were employed. MANOVA is an extension of the univariate analysis of variance (ANOVA). An ANOVA includes the examination of statistical differences of one continuous dependent variable to an independent grouping variable. The MANOVA extends the ANOVA by considering multiple continuous dependent variables and packages them together into a subjective undeviating composite variable. The MANOVA indicates whether the newly created composite variable differs between the different groups, of the independent variable. Essentially, the MANOVA determines whether the independent grouping variable simultaneously simplified a statistically significant amount of variance in the dependent variable. The MANOVA was conducted using the Procrustes ANOVA function on the R-package geomorph in R [22]. 50-50 MANOVA [23] is a modified form of a MANOVA, designed for many response variables that are possibly associated. The 50-50 MANOVA was conducted using the R packages fmanova [24]. For accuracy purposes, permutation tests (non-parametric tests) were used to double-check the results. Permutation testing is based on resampling and has less statistical power than parametric testing. The function allowed shape variation attributable to the sex factor to be quantified in a linear model and estimated the

significant likelihood of this variation for a null model through distributions generated from resampling permutations. The chosen factor (sex) was calculated and compared to values obtained from the sample, randomly and repeatedly assigned. The number of resampled values that surpassed the "true" value was divided by the total number of permutation rounds (10 000 rounds). The null hypothesis could not be rejected if the value fell within the range of random grouping and if the measurement values do not exceed the one generated by chance [25], [26], [27]. Permutation testing was conducted using the morpho R-packages [27]. Thereafter, for sex classification purposes and to assess the discriminant power of sex, standard Discriminant Function Analysis (DFA) was performed on the PCs, and the results were validated using leave-one-out cross-validation [26,27]. DFA locates linear groupings of variables that describe differences between groups. These groupings define discriminant functions. DFA was performed using the morpho R-packages [27].

All statistical analyses performed in this study were done on R-studio v 1.0.44-®2009-2016 for Windows [28].

Results

For the placement of the 18 anatomical landmarks, the dispersion means ($\mu \Delta$) values for both the automatic and manual landmarking procedures were 1.92mm (SD 0.64) and 1.93mm (SD 1.51) for INTRA-OE, and 2.13mm (SD 0.85) and 1.04mm (SD 1.28) for INTER-OE, respectively (Table 3). For the automatic placement of the anatomical landmarks, the right anterior superior iliac spine (landmark 2), right anterior inferior iliac spine (landmark 4), both iliac crests (landmarks 7 and 8), right ischial spine (landmark 10), distal point of the ischial tuberosity (landmarks 13 and 16), and arcuate line (landmarks 17 and 18) were prone to more INTER-OE. For the manual placement of the anatomical landmarks, the ischial tuberosity (landmarks 13 and 16) was prone to more INTER-OE, while both iliac crests (landmarks 7 and 8), ischial spines (landmarks 9 and 10), and both inferior points of the ischial tuberosity (landmarks 12 and 15) were prone to more INTRA-OE. The dispersion mean values for the INTRA-OE and INTER-OE were relatively smaller for the automatic placement of landmarks as compared to manual placement (Fig. 3). Higher INTER-OE were observed for the automatic placement of landmarks while higher INTRA-OE were observed for manual landmark placement.

Table 3. Dispersion errors (mm) of pelvis landmarks and sliding landmarks positioned on CT scans using the automatic and manual landmarking methods.

	Intra-observer errors				Inter-observer errors			
	Automatic		Manual		Automatic		Manual	
	Mean	SD	Mean	SD	Mean	SD	Mean	SD
Curve1	2.30	0.34	4.13	2.87	2.13	0.83	2.64	2.98
Curve2	1.95	0.56	2.58	1.68	2.47	0.88	1.13	1.69
Curve3	1.74	0.75	2.01	1.66	2.18	0.69	2.23	1.93
Curve4	1.15	0.29	3.10	1.21	3.48	0.82	2.25	1.33
Landmarks	1.92	0.64	1.93	1.51	2.13	0.85	1.04	1.28

*Curve 1= left greater sciatic notch, curve 2= right greater sciatic notch, curve 3= left ischiopubic ramus, curve 4= right ischiopubic ramus Mean is the dispersion mean value. SD is the standard deviation. Dispersion mean values < 2 mm indicate a high level of reliability and repeatability of both landmarking methods.

Intra- and inter-observer errors for the placement of 260 sliding landmarks were calculated using both landmarking procedures , and are shown in Table 3 and illustrated in Fig. 4. For the

placement of 68 sliding landmarks on curve 1 (left greater sciatic notch), lower dispersion mean ($\mu \Delta$) values were observed for the automatic landmarking method. For the placement of 68 sliding landmarks on curve 2 (right greater sciatic notch), lower dispersion mean values were obtained for the automatic landmarking method on curve 2. However, a high dispersion means ($\mu \Delta$) value was observed for the automatic method in terms of INTER-OE (Fig. 4). For the placement of 62 sliding landmarks on curve 3 (left ischiopubic ramus), lower dispersion values were obtained for the automatic placement of sliding landmarks (Fig. 4). Lastly, for the automatic and manual placement of 62 sliding landmarks on curve 4, lower dispersion mean ($\mu \Delta$) values were obtained for the automatic placement of sliding landmarks on curve 4. However, a higher dispersion means ($\mu \Delta$) value was observed for the automatic method in terms of INTER-OE (Fig. 4).

In general, high INTRA-OE and INTER-OE were observed for the manual placement of anatomical and sliding landmarks. In addition, lower dispersion mean ($\mu \Delta$) values were obtained for the automatic placement of anatomical and sliding landmarks.

In terms of variance analysis, the presence of sexual dimorphism was confirmed through the observation of significant p-values (< 0.05) when using both landmarking procedures. In addition, cross-validated discriminant function analysis yielded an accuracy of 83% (curve 1), 98% (curve 2), 84% (curve 3), 95% (curve 4), and 98% (anatomical landmarks) for automatic landmark placement, and an accuracy of 68% (curve 1), 66% (curve 2), 70% (curve 3), 67% (curve 4), and 93% (landmarks) for manual landmark placement. These results indicated the discriminative power of sexual dimorphism that can be reflected by the automatic method compared to manual landmarking which provided lower accuracy rates (66% - 93%) relative to the automatic landmarking method (83% - 98%). The effect of sex on pelvic shape was statistically significant (Table 4), indicating that sex contributes to the overall shape variation of the pelvis which was better reflected using the automatic landmarking method. All parametric (MANOVA) and nonparametric (50-50 MANOVA) tests reported significant pelvis shape differences attributed to sex differences between males and females with significantly lower p-values observed for the automatic placement of landmarks. For the greater sciatic notch, an accuracy of 90% was achieved using the automatic method, while an accuracy of 67% was achieved using the manual method. Similarly, an accuracy of 90% and 69% was achieved for the ischiopubic ramus when using the automatic semi-landmarking and manual methods respectively.

Table 4. Sex shape analysis results.

	Automatic				Manual			
	MANOVA	50-50 MANOVA	PERM	DFA	MANOVA	50-50 MANOVA	PERM	DFA
Curve1	0.001**	3.19e-11***	0.001	82.95	0.007**	0.000764***	0.006	68.18
Curve2	0.001**	<2e-16***	0.001	97.73	0.035*	0.00196**	0.034	65.91
Curve3	0.001**	<2e-16***	0.001	84.09	0.001**	2.01e-05***	0.001	70.45
Curve4	0.001**	<2e-16***	0.001	95.45	0.004**	0.00232**	0.002	67.05
Landmarks	0.001**	<2e-16***	0.001	97.73	0.001**	<2e-16***	0.001	93.18

Significant p-values (<0.05) are indicated in bold. ** = p-values less than 0.01 and *** = p-values less than 0.001.

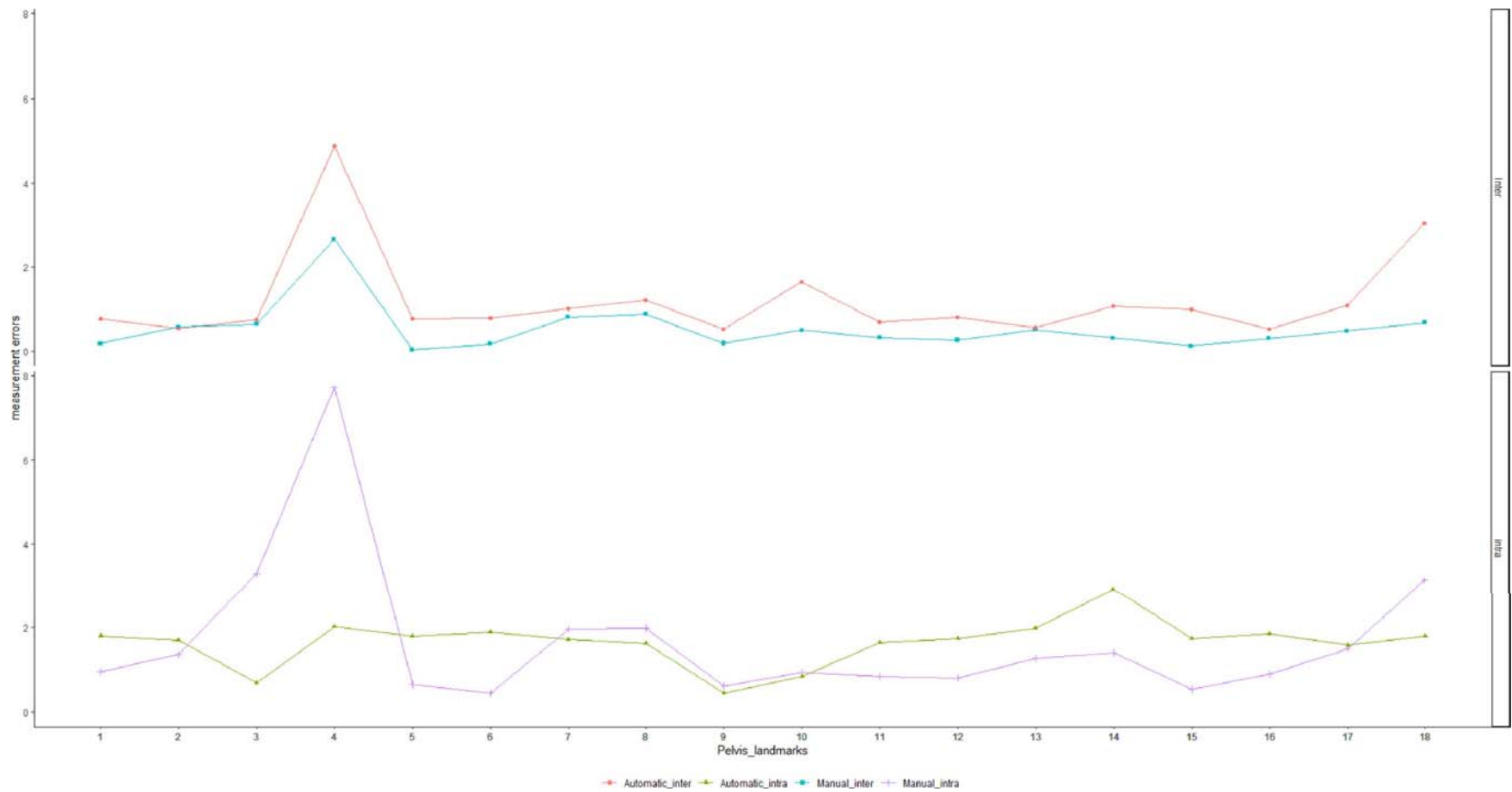


Fig. 3. Graphical comparison between the mean standard error results for both intra- (bottom) and inter-observer (top) errors of the automatic and manual placement of anatomical landmarks.

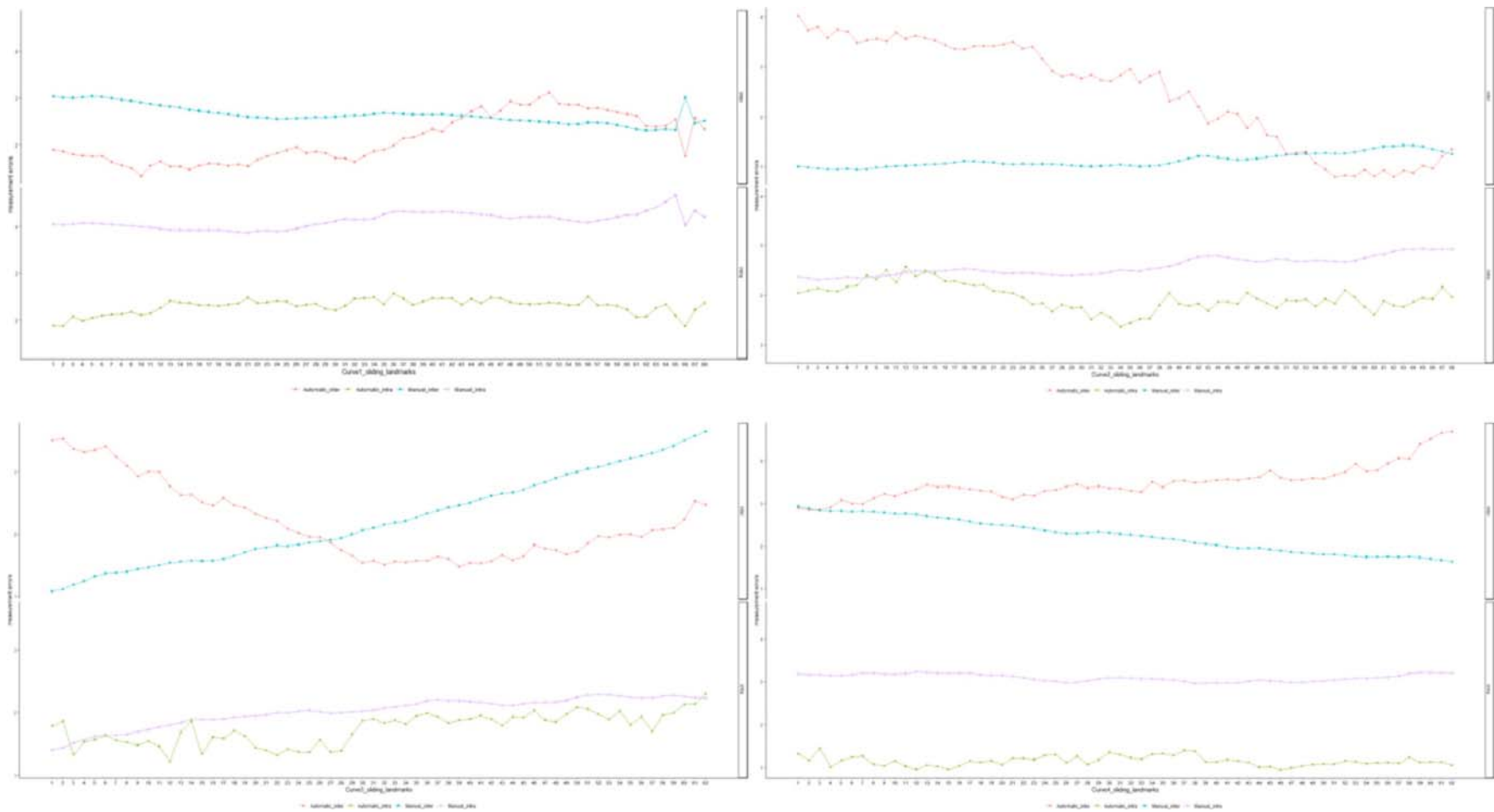


Fig. 4. Graphical comparison between the mean, standard error results for both intra- and inter-observer errors of the positioning of the sliding landmarks (curve 1, curve 2, curve 3, and curve 4) using the automatic and manual semi-landmarking methods.

Discussion

This study aimed to validate the utilisation of the automatic placement of anatomical and sliding landmarks on 3D models for shape analysis of human pelvis. The reconstruction of 3D pelvis models and shape analysis were acquired using both manual and automatic landmarking procedures and compared using reproducibility testing of landmarks and GMM.

The results obtained in this research study validated the accuracy and precision of the automatic placement of anatomical and sliding landmarks on 3D surfaces of pelvic elements. Furthermore, it indicated that the automatic placement of landmarks reduces intra- and inter-observer errors, with lower dispersion mean ($\mu \Delta$) values observed for the automatic placement of both anatomical and sliding landmarks. Finally, the application of GMM has proven to be a valuable alternative to quantify sexual dimorphism in the shape of the greater sciatic notch and ischiopubic region. This was corroborated by higher classification accuracy rates observed for the shape variables compared to manual methods, indicating that the automatic placement of sliding landmarks displays marked sex differences in pelvic shape morphology.

Automatic landmark placement on the right anterior iliac spine, right anterior inferior iliac spine, both iliac crests, right ischial spine, distal point of the ischial tuberosity, and arcuate line were prone to more inter-observer errors, while manual landmark placement on the ischial tuberosity were prone to more inter-observer errors. The manual placement of landmarks on the iliac crests, ischial spines, and inferior point of the ischial tuberosity was prone to more intra-observer errors. The errors mentioned above in the results were inconsistent with results obtained from other studies [16,29]. The errors observed in positioning these landmarks may be due to the inexperience of the observer or perhaps due to the different modalities used. In addition, the automatic landmarking procedure is best suitable for large datasets. Consequently, the errors observed are not significant to warrant not using the data for further analysis as both landmarking methods have proven to be reliable, but the automatic method proved to be less prone to human error in landmark placement.

Regarding the automatic positioning of sliding landmarks on curve 1, lower dispersion means ($\mu \Delta$) values were obtained compared to manual placement, with lower intra- and inter-observer errors observed for automatic placement. Lower dispersion means ($\mu \Delta$) values were also observed for the automatic placement of sliding landmarks on curves 2, 3, and 4. However, for curves 2 and 4, the automatic placement of sliding landmarks obtained high dispersion mean ($\mu \Delta$) values in terms of inter-observer errors. In this study, reduced (or lower) intra- and inter-observer errors were obtained using the automatic method, which was represented by lower dispersion mean ($\mu \Delta$) values. This indicates that the automatic placement of landmarks provides better repeatability and consistency as less variation was observed in the automatic placing of landmarks than the manual method. This is consistent with other studies [10,11].

Shape analysis of the pelvis, specifically of the greater sciatic notch and ischiopubic ramus, revealed statistically significant differences between the sexes for both the automatic and manual landmarking methods, confirming the expression of sexual dimorphism in the pelvis. These results are consistent with previous studies [16] which have demonstrated that the ischiopubic region and great sciatic notch can represent sex-based variations of the pelvic bone. In addition, cross-validated discriminant function analysis yielded greater accuracy rates for the automatic placement of landmarks compared to manual positioning, indicating that sexual dimorphism is better reflected using the automatic landmarking procedure. The findings show

that sex differences between males and females play an important role in the overall shape variation of the human bony pelvis.

There are dramatic functional differences between the male and female pelvic anatomy [30,31]. These extend to the bony skeleton and represent differences found in all modern human groups, which were reflected by the statistically significant p-values observed in Table 4. The greater sciatic notch and ischiopubic ramus have been shown to display sex differences between males and females. Males typically display a narrow notch, while females display a broader, obtuse notch [30,31]. The ischiopubic ramus is narrow and sharp in females, whereas it is broad and rounded in males. However, these shape differences are not as reliable as those observed in the subpubic region and should be thought of as secondary indicators in the absence of the other two criteria- ventral arc and subpubic concavity of the Phenice traits [32]. Nonetheless, the use of the automatic placement of sliding landmarks on these two curves permitted us to visualize morphological changes or differences in the pelvis shape (because of sex) with the use of standard DFA whereby higher classification accuracy rates were obtained for the automatic placement of sliding landmarks regarding sexual dimorphism. In addition, the study showed that the utilisation of multivariate statistical analysis of sliding landmarks placed on the greater sciatic notch and ischiopubic regions allows for the quantification of sex differences between males and females.

Imaging techniques such as CT have progressed greatly, allowing researchers to generate highly accurate models and reconstructions from skeletal elements. The reconstruction of 3D models from surface scans has become common in forensic science. Numerous studies [33], [34], [35], [36], [37] have confirmed the reproducibility of 3D-CT images of the skeletonised bony pelvis and their applicability to anthropological measurements. Three-dimensional surfaces of the pelvis produce well-curved features that facilitate computerised geometrical analyses. Geometric morphometrics enables the analysis of curved structures such as the greater sciatic notch and ischiopubic ramus of the pelvis, which have successfully demonstrated sexual dimorphism in this study and numerous others [5,36,37]. When comparing the results of this study to other studies [5,36,37], the multivariate analysis of anatomical and sliding landmarks on the ischiopubic-region and greater sciatic notch allowed for the examination of sexual dimorphism between the sexes with higher accuracy rates observed when using the automatic landmarking method. Additionally, the analysis of the morphology of the greater sciatic notch and ischiopubic ramus by placing sliding landmarks automatically has proven that this method has the potential to become a reliable and accurate technique for sex estimation. Moreover, the coordinates of the anatomical and sliding landmarks can be digitized by the observers with little to no experience when analysing pelvic sexual dimorphism. Although the pubic bone is regarded as one of the most dimorphic structures in the skeleton, it is also one of the worst preserved parts of the skeleton in buried contexts. Therefore, pelvic shape analysis of the greater sciatic notch and ischiopubic regions will be beneficial to forensic anthropologists. This study has shown that a sliding landmark-based analysis, especially automatically of the greater sciatic notch provides relatively high accuracies for sex estimation, around 90% (Table 4).

In addition to reducing measurement errors, this research study demonstrates applying the automatic landmarking method on 3D surfaces of pelvic elements as a convenient prerequisite for geometric morphometrics-based shape analysis of the bony pelvis. New 3D imaging methods might allow forensic analysts to assess specific sexual dimorphism patterns not readily revealed by non-metric and metric methods. Recently, Braun and collaborators [38] successfully applied the automatic method for the analysis of the hard-tissue menton shape

variation in adult South Africans using CBCT scans. However, the automatic placement of landmarks needs to be applied on additional 3D surfaces of different anatomical elements before it can be robust. In this study, we provided an overview of the influence of sex on the variability of the human bony pelvis, however, the influence of other factors such as population affinity and age were not included in this study. When developing approaches using the automatic landmarking method, it may be useful to consider additional factors such as population affinity and age to enhance the accuracy of the method further. In addition, population affinity has been a critical component of shape variation whereby the degree and pattern of expression of sexual dimorphism varies across populations [39,40]. Therefore, the incorporation of population affinity should be considered as an avenue for future studies to test for differences between and among South African populations regarding sexual dimorphism using geometric morphometric methods. For this study, CT scans were used which may have served as a limitation because a disadvantage of CT datasets is the inclusion of lower spatial resolution and isotropic volumetric data for the accurate positioning of 3D landmarks [10].

Conclusion

This study provides validation for the utilisation of the automatic placement of anatomical and sliding landmarks on pelvic elements. The automatic positioning of landmarks and sliding landmarks on 3D surfaces increases objectivity and reliability. In addition to the automatic landmarking method providing lower intra- and inter-observer errors compared to manual landmarking, the method allows us to achieve better precision.

A reliable method for sex estimation should maximise both accuracy and precision to achieve reliable results between observers and high rates of correct classifications. In this research, the automatic positioning of anatomical and sliding landmarks has proven to be a highly reliable method for estimating sex based on shape differences on the pelvis. In addition, the integration of sliding landmarks enables us to describe and visualise skeletal structures more satisfactorily. The automatic placement of anatomical and sliding landmarks can be highly replicable and applied by observers with different experience levels in estimating sex and overall.

Declaration of Competing Interest

The authors declare that they have no known competing financial interests or personal relationships that could have appeared to influence the work reported in this paper.

Acknowledgments

We acknowledge Suvasha Jagesur (previous researcher) for granting us permission to use the scans from the Radiology department at Steve Biko Academic Hospital. Ethical clearance to conduct this research was obtained from the Faculty of Health Sciences Research Ethics committee of the University of Pretoria (Ethics Reference No:253/2021). We acknowledge Bakeng se Afrika, coordinated by Prof. Ericka N. L'Abbé (University of Pretoria, Pretoria, South Africa) and Prof. Anna Oetlé (Sefako Makgatho Health Sciences University, Ga-Rankuwa, Pretoria, South Africa) for the financial support.

References

- [1] E.N. L'Abbé, M. Loots, J.H. Meiring, The Pretoria bone collection: a modern South African skeletal sample, *HOMO* 56 (2005) 197–205, <https://doi.org/10.1016/j.jchb.2004.10.004>.
- [2] M. Zuzile, TimesLive-2021. <https://www.timeslive.co.za/news/south-africa/2021-03-15-more-than-1000-unidentified-bodies-lying-in-gauteng-mortuaries/>. Accessed 24 April 2022.
- [3] G.C. Krüger, E.N. L'Abbé, K.E. Stull, M.W. Kenyhercz, Sexual dimorphism in cranial morphology among modern South Africans, *Int. J. Legal Med.* 129 (2015) 869–875, <https://doi.org/10.1007/s00414-014-1111-0>.
- [4] G.C. Krüger, E.N. L'Abbé, K.E. Stull, Sex estimation from the long bones of modern South Africans, *Int. J. Legal Med.* 131 (2017) 275–285, <https://doi.org/10.1007/s00414-016-1488-z>.
- [5] K. Krishan, P.M. Chatterjee, T. Kanchan, S. Kaur, N. Baryah, R.K. Singh, A review of sex estimation techniques during examination of skeletal remains in forensic anthropology casework, *Forensic Sci. Int.* 261 (2016) 165, <https://doi.org/10.1016/j.forsciint.2016.02.007>, e1-165.e8.
- [6] E.N. L'Abbé, M. Kenyhercz, K.E. Stull, N. Keough, S. Nawrocki, Application of Fordisc 3.0 to explore differences among crania of North American and South African blacks and whites, *J. Forensic Sci.* 58 (2013) 1579–1583, <https://doi.org/10.1111/1556-4029.12198>.
- [7] A.R. Klales, S.D. Ousley, J.M. Vollner, A revised method of sexing the human innominate using Phenice's nonmetric traits and statistical methods, *Am. J. Phys. Anthropol.* 149 (2012) 104–114, <https://doi.org/10.1002/ajpa.22102>.
- [8] F.L. Bookstein, *Morphometric Tools For Landmark Data: Geometry And Biology*, 1st pbk, Cambridge University Press, Cambridge [England], 1997.
- [9] N.R. Langley, L.M. Jantz, S.D. Ousley, R.L. Jantz, G. Milner, *Data Collection Procedures For Forensic Skeletal Material 2.0*, University of Tennessee and Lincoln Memorial University, 2016.
- [10] A. Ridel, F. Demeter, M. Galland, E. L'Abbé, D. Vandermeulen, A. Oettlé, Automatic landmarking as a convenient prerequisite for geometric morphometrics. Validation on cone beam computed tomography (CBCT)- based shape analysis of the nasal complex, *Forensic Sci. Int.* 306 (2020), 110095, <https://doi.org/10.1016/j.forsciint.2019.110095>.
- [11] A.F. Ridel, et al., Nose approximation among South African groups from cone-beam computed tomography (CBCT) using a new computer-assisted method based on automatic landmarking, *Forensic Sci. Int.* 313 (Aug. 2020), 110357, <https://doi.org/10.1016/j.forsciint.2020.110357>. DOI.org (Crossref).
- [12] C.F. Spoor, F.W. Zonneveld, G.A. Macho, Linear measurements of cortical bone and dental enamel by computed tomography: Applications and problems, *Am. J. Phys. Anthropol.* 91 (1993) 469–484, <https://doi.org/10.1002/ajpa.1330910405>.

- [13] C.A. Schneider, W.S. Rasband, K.W. Eliceiri, NIH Image to ImageJ: 25 years of image analysis, *Nat Methods* 9 (2012) 671–675, <https://doi.org/10.1038/nmeth.2089>.
- [14] P. Claes, A robust statistical surface registration framework using implicit function representations: Application in craniofacial reconstruction. PhD Thesis, K.U. Leuven, Belgium 2007.
- [15] M.C.M. Fischer, F. Krooß, J. Habor, K. Radermacher, A robust method for automatic identification of landmarks on surface models of the pelvis, *Sci Rep* 9 (2019) 13322, <https://doi.org/10.1038/s41598-019-49573-4>.
- [16] H.I. Robertson, D.L. Pokotylo, D.A. Weston, Testing landmark redundancy for sex-based shape analysis of the adult human os coxa, *Am J Phys Anthropol* (2019) ajpa.23860, <https://doi.org/10.1002/ajpa.23860>.
- [17] D.E. Slice, Geometric Morphometrics, *Annu. Rev. Anthropol.* 36 (2007) 261–281, <https://doi.org/10.1146/annurev.anthro.34.081804.120613>.
- [18] I.L. Dryden, K.V. Mardia, Statistical shape analysis with applications in R, Second edition, John Wiley & Sons, Chichester, UK; Hoboken, NJ, 2016.
- [19] J.C. Gower, Generalized procrustes analysis, *Psychometrika* 40 (1975) 33–51, <https://doi.org/10.1007/BF02291478>.
- [20] F.J. Rohlf, D. Slice, Extensions of the Procrustes Method for the Optimal Superimposition of Landmarks, *Systematic Zoology* 39 (1990) 40, <https://doi.org/10.2307/2992207>.
- [21] L. Scrucca, Assessing Multivariate Normality Through Interactive Dynamic Graphics, (2000).
- [22] R: Geometric Morphometric Analyses of 2D/3D Landmark Data, (n.d.). <https://search.r-project.org/CRAN/refmans/geomorph/html/00Index.html> (accessed December 8, 2022).
- [23] O. Langsrud, 50-50 multivariate analysis of variance for collinear responses, *J R Statist Soc D* 51 (2002) 305–317, <https://doi.org/10.1111/1467-9884.00320>.
- [24] O. Langsrud, B.H. Mevik, Fifty-fifty MANOVA in `ffmanova`; 2012.
- [25] S. Schlager, Soft-Tissue Reconstruction of The Human Nose: Population Differences And Sexual Dimorphism=Weichteilrekonstruktion Der Menschlichen Nase: Populationsunterschiede Und Sexualdimorphismus[dissertation], Universtat Freiburg, Freiburg im Breisgau, Germany, 2013.
- [26] S. Schlager, A. Rüdell, Analysis of the human osseous nasal shape-population differences and sexual dimorphism: human osseous nasal shape, *Am. J. Phys. Anthropol.* 157 (2015) 571–581, <https://doi.org/10.1002/ajpa.22749>.
- [27] S. Schlager, Jefferis G, Dryden IL. Calculations and visualisations related to Geometric Morphometrics; 2020.

- [28] R a Language and Environment for Statistical Computing: Reference Index, R Foundation for Statistical Computing, Vienna, 2010.
- [29] J.A. Bytheway, A.H. Ross, A geometric morphometric approach to sex determination of the human adult Os Coxa: a geometric morphometric approach to sex determination, *J. Forensic Sci.* 55 (2010) 859–864, <https://doi.org/10.1111/j.1556-4029.2010.01374.x>.
- [30] P.L. Walker, Greater sciatic notch morphology: Sex, age, and population differences, *Am. J. Phys. Anthropol.* 127 (2005) 385–391, <https://doi.org/10.1002/ajpa.10422>.
- [31] J. Bruzek, A method for visual determination of sex, using the human hip bone, *Am. J. Phys. Anthropol.* 117 (2002) 157–168, <https://doi.org/10.1002/ajpa.10012>.
- [32] D. Dirkmaat, *A Companion To Forensic Anthropology*, Wiley-Blackwell, Malden, MA, 2012.
- [33] H. Biwasaka, Y. Aoki, K. Sato, T. Tanijiri, S. Fujita, K. Dewa, K. Yoshioka, M. Tomabechei, Analyses of sexual dimorphism of reconstructed pelvic computed tomography images of contemporary Japanese using curvature of the greater sciatic notch, pubic arch and greater pelvis, *Forensic Sci. Int.* 219 (2012) 288, <https://doi.org/10.1016/j.forsciint.2011.11.032>, e1-288.e8.
- [34] O.A. Arigbabu, I.Y. Liao, N. Abdullah, M.H. Mohamad Noor, Computer vision methods for cranial sex estimation, *IPSN T Comput. Vis. Appl.* 9 (2017) 19, <https://doi.org/10.1186/s41074-017-0031-6>.
- [35] L.A.B. Wilson, L.T. Humphrey, voyaging into the third dimension: A perspective on virtual methods and their application to studies of juvenile sex estimation and the ontogeny of sexual dimorphism, *Forensic Sci. Int.* 278 (2017) 32–46, <https://doi.org/10.1016/j.forsciint.2017.06.016>.
- [36] E. Pretorius, M. Steyn, Y. Scholtz, Investigation into the usability of geometric morphometric analysis in assessment of sexual dimorphism, *Am. J. Phys. Anthropol.* 129 (1) (2006) 60–64.
- [37] P.N. Gonzalez, V. Bernal, S.I. Perez, Geometric morphometric approach to sex estimation of human pelvis, *Forensic Sci. Int.* 189 (2009) 68–74, <https://doi.org/10.1016/j.forsciint.2009.04.012>.
- [38] S. Braun, A.F. Ridel, E.N. L'Abbé, A.C. Oettlé, Analysis of the hard-tissue menton shape variation in adult South Africans using cone-beam computed tomography (CBCT) scans, *Forensic Imaging* 32 (2023), 200532, <https://doi.org/10.1016/j.fri.2023.200532>.
- [39] P.L. Walker, Sexing skulls using discriminant function analysis of visually assessed traits, *Am. J. Phys. Anthropol.* 136 (2008) 39–50, <https://doi.org/10.1002/ajpa.20776>.
- [40] I. Ari, Morphometry of the greater sciatic notch on remains of male Byzantine skeletons from Nicea, *Eur. J. Anatomy* 9 (2005) 61–165.